Effect of pH and Ligand Binding on the Structure of the Cu Site of the Met121Glu Mutant of Azurin from *Pseudomonas aeruginosa*

Richard W. Strange,[‡] Loretta M. Murphy,[‡] B. Göran Karlsson,[§] Bengt Reinhammar,[§] and S. Samar Hasnain*[,‡]

Molecular Biophysics Group, CCLRC Daresbury Laboratory, Warrington WA4 4AD, Cheshire, U.K., and Department of Biochemistry and Biophysics, Chalmers University of Technology and Göteborg University, Göteborg, Sweden

Received July 10, 1996; Revised Manuscript Received October 15, 1996[⊗]

ABSTRACT: A pH-dependent X-ray absorption fine structure (XAFS) study has been undertaken to provide a structural interpretation of the spectroscopic properties of the Met121Glu mutant of azurin from *Pseudomonas aeruginosa* (Az_p). Ligand binding studies have been carried out to investigate the effect of the cavity formed at the Cu site as a result of the mutation. The optical spectrum at pH 4 exhibits an intense band at ∼600 nm and a weaker band at ∼450 nm, typical for the blue copper proteins. As the pH is increased, these bands decrease in intensity and shift to 570 and 413 nm, respectively, with the latter becoming the more intense of the two [Karlsson, B. G., et al. (1991) *Protein Eng. 4* (3), 343−349]. These changes are accompanied by a change in the EPR spectrum from a rhombic type 1 Cu spectrum at pH 4 to a spectrum with the rhombic splitting decreasing to zero and the hyperfine coupling increasing from 25 to 83 G. X-ray absorption at the Cu K-edge shows that this change results from the lengthening of the Cu−His (by 0.07 Å) and Cu−Cys (by 0.06 Å) bonds and the coordination of one of the oxygen atoms of the glutamate ligand at pH 8, at a distance as close as 1.90 Å. The copper site thus changes from a normal type 1 copper center with three strong bonds at pH 4 to a copper site with four strong bonds at pH 8, with Cu−His distances significantly longer than known distances for type 1 copper centres measured using the XAFS technique. The XAFS of the azide derivative measured at pH 8 shows a similar Cu coordination, with azide replacing glutamate as the fourth ligand. Azide binding at pH 8 is accompanied by a further increase in the EPR hyperfine coupling to 110 G. This structural information when taken together with recent structural sudies on copper proteins points toward the need for a reexamination of the basis on which copper proteins are classified.

Type 1 (or "blue") single-copper proteins are characterized by their unusual spectroscopic properties, which include a high-intensity electronic absorption band at ∼600 nm and a small magnetic hyperfine splitting (<90 G) in the $g_{||}$ region of the electron paramagnetic resonance (EPR) spectrum (Malkin & Malmström, 1970). They also possess an unusually strong oxidizing power, which ranges from 184 mV for stellacyanin from *Rhus vernicifera* to 680 mV for rusticyanin from *Thiobacillus Ferro-oxidans* (Adman, 1985). The same basic coordination to the Cu(II) atom is present in all type 1 copper proteins. This consists of an inner coordination sphere of two histidine ligands and a cysteine ligand. In azurin, plastocyanin, and cucumber basic protein, a fourth, more distant ligand is supplied by a sulfur from a methionine residue (Adman & Jensen, 1981; Norris et al., 1986; Baker, 1988; Guss & Freeman, 1983; Guss et al., 1988; Fields et al., 1991). In azurin, a distant fifth ligand is supplied by an oxygen from a glycine residue (Baker, 1988; Nar et al., 1991; Dodd et al., 1995). In stellacyanin, there are no methionine residues (Bergman et al., 1977) and the identity of any fourth copper ligand is uncertain, although recent studies have suggested that it might be a glutamine side chain (Fields et al., 1991; Thomann et al., 1991; Strange et al., 1995). There remains a considerable interest in how the same basic ligation at the copper center is "fine tuned" to produce such a wide range of reduction potentials. In particular, the role of methionine, or another fourth ligand, has been extensively discussed in terms of a fine-tuning mechanism (Gray & Malmström, 1983; Guss et al., 1986).

In recent years, site-directed mutagenesis has provided a means of selectively replacing or deleting residues, or sequences of residues, in the type 1 copper proteins (Karlsson et al., 1989a; Canters, 1987). In the present paper, we have extended this study to examine the properties of the copper site of azurin where the Met-121 ligand has been replaced by glutamic acid, to give a mutant Met121Glu. This mutant is particularly interesting in that its electronic absorption spectrum shows a strong pH dependence, suggested to be due to the titration of the glutamate side chain (Karlsson et al., 1991). At pH 4, there is an intense absorption at ∼600 nm, typical for type 1 copper proteins with a rhombic EPR spectrum. Upon raising of the pH, this absorption band undergoes a blue shift while the 450 nm band shifts to 413 nm and becomes the stronger of the two. The protein solution changes from blue to brown at pH 8. The EPR spectrum changes from the rhombic type 1 Cu spectrum and exhibits a hyperfine coupling A_z of 83 G, and $g_x = g_y =$ 2.06 and $g_z = 2.3$, very similar to the catalytic Cu site of blue nitrite reductase (NiR) (Howes et al., 1994).

We have used the XAFS to examine the structure of the copper center of the Met121Glu mutant at pH 4 and 8 in order to provide direct structural information around the Cu site with the aim of providing a structural explanation for the optical absorbance and EPR changes at the Cu center.

[‡] Daresbury Laboratory.
[§] Chalmers University of Technology and Göteborg University.
[⊗] Abstract published in *Advance ACS Abstracts,* November 15, 1996.

S0006-2960(96)01682-0 CCC: $12.00

Azide binding at pH 8 has been investigated by both EPR and the XAFS to shed light on the cavity which might be created at the Cu site in the mutant protein.

MATERIALS AND METHODS

Materials. All chemicals were reagent grade and used without further purification. Water was deionized using an Elgastat Water treatment system. The buffer system used for the experiments at pH 8 was 20 mM *N*-(2-hydroxyethyl)-piperazine-*N*′-2-ethanesulfonic acid or HEPES. Experiments at pH 4 were carried out using 20 mM sodium acetate buffer. All protein manipulations were performed at 4 °C unless otherwise stated. Final stage concentrations were performed using Centricon-10 concentrators from Amicon Ltd.

Expression of Azurin and Site-Directed Mutagenesis of the Met-121 Residue. Az_p was expressed in *Escherichia coli* as described elsewhere (Karlsson et al., 1989b, 1991). In the purification of the wild type protein, an anionic exchange chromatography step was included (van de Kamp et al., 1990) and the absorbance ratio of the wild type was 0.61. In the purification of the mutant protein, this step results in partial loss of copper. The absorbance ratio of Met121Glu was 0.34 at pH 4 (613/280) and 0.19 at pH 8 (413/280).

Optical and EPR Spectroscopy. Absorption spectra of Met121Glu in the optical region were measured and compared with the published data (Karlsson et al., 1991) to check the sample integrity before and after XAFS data collection. The optical spectrum for the azide-bound derivative was recorded under similar conditions. One milliliter of 2.13×10^{-4} M Met121Glu in 20 mM HEPES buffer at pH 8 was titrated with 10 μL aliquots of 1 M NaN_3 in 20 mM HEPES buffer at pH 8 until a total of 140 μL had been added. After each addition, the sample was thoroughly mixed and the visible spectrum recorded. Approximately 650 equiv of NaN_3 was added to Met121Glu with only minor changes in the shape and position of the absorption bands. The spectra were recorded over the range of 350−900 nm on a Phillips Series PU 8700 single-beam spectrometer or Perkin-Elmer Lambda 16 UV/Vis spectrometer.

EPR spectra were recorded at the X-band at 77 K on a JEOL JES-RE2X spectrometer or on a Varian E-3 spectrometer. For the azido derivative, 100 μL of 6.13 mM Met121Glu in 20 mM HEPES buffer at pH 8 was titrated with small aliquots of 2 M NaN_3 in 20 mM HEPES buffer at pH 8 until a total of 75 μL had been added. After each addition, the sample was thoroughly mixed and the EPR spectrum recorded. Addition of sodium azide initially changed the EPR spectrum from that typical of Met121Glu at pH 8 to a spectrum which indicated the presence of more than one species of copper. As the amount of sodium azide was increased, the proportion of the EPR spectrum attributable to the new species, Met121Glu−azide, increased. Final spectra were obtained on sample with a total of 75 μL of 2 M NaN_3 at pH 8 (244 equiv per copper). No further change in the EPR spectrum was observed after the addition of 39 μL of 2 M NaN_3 (127 equiv per copper).

X-ray Absorption Spectroscopy. All protein samples were concentrated to a volume of ca. 0.25 mL to give copper concentrations of 1−3 mM. The samples were placed in Perspex XAFS cells, with Mylar windows, and frozen in liquid nitrogen. The XAFS cell window dimensions were $8 \times 10 \times 2$ mm (height × width × depth). XAFS data was recorded in the fluorescence mode at the Cu K-edge using either the 5T superconducting wiggler station 9.2 or dipole station 8.1 at the Synchrotron Radiation Source (SRS), Daresbury Laboratory, U.K. The SRS was operating at an energy of 2.0 GeV with an average current of 150 mA and a beam lifetime in excess of 20 h. An order-sorting Si(220) double-crystal monochromator was used to reduce harmonic contamination in the monochromatic beam. Extended X-ray absorption fine structure (EXAFS) data were collected on station 9.2 using a beam size of 3×5 mm (height × width). X-ray absorption near-edge structure (XANES) data were recorded using a focused monochromatic beam on station 8.1.[1] All protein samples were cooled to 77 K through the use of a liquid nitrogen cryostat. A 13-element germanium solid state detection system was employed, allowing high-quality fluorescence XAFS data to be recorded. A standard 5 mM $CuSO_4$ solution was used to isolate the Cu K-edge fluorescence signal from the scattered X-rays when setting up the solid state detector system. The X-ray energy was calibrated by measuring the edge spectrum of Cu foil in transmission mode and setting the first inflection point at 8982 eV.

An average of 8−12 scans were recorded per sample. For each sample, the individual scans were examined and each detector element was weighted relative to the edge height and then summed using the Daresbury Laboratory program EXCALIB (Morrell et al., 1989). Background subtraction and normalization was performed using the Daresbury Laboratory program EXBACK (Morrell et al., 1989).

The Daresbury Laboratory program EXCURV92 (Binsted et al., 1991, 1992) was used for data analysis, employing fast curved wave single- and multiple-scattering theory (Gurman et al., 1984, 1986) on k^3-weighted EXAFS data. The Cu, N, C, and O phase shifts were calculated using the program MUFPOT, and the S phase shift was obtained from EXCURV92, which uses a simplified version of the MUFPOT program. Details of the procedure used are given elsewhere (Binsted et al., 1987). The phase shifts have previously been used to fit a number of copper−histidine/pyridine model compounds and the EXAFS of several type 1 Cu proteins (Strange et al., 1987, 1995a,b; Blackburn et al., 1988; Murphy et al., 1993; Grossmann et al., 1995). The photoelectron energy threshold value, E_0, was treated as a single overall parameter for the multiple-shell fit. This has been found adequate for systems where the backscatterers are all of a similar nature. The quality of the theoretical simulations was determined by a visual comparison of the EXAFS and Fourier transforms and by the fit index (FI) and *R* factor (*R*), as described in Binsted et al. (1992). Constrained and restrained refinement procedures (Hasnain, 1988; Binsted et al., 1992) were used to reduce the number of free parameters in the least-squares refinement. The application of this procedure to type 1 Cu proteins has been described in detail in Strange et al. (1995a). The imidazole of the histidine ligand requires six parameters, the cysteine sulfur two parameters, the glutamate six parameters, and the azide five parameters. Thus, simulations involved a maximum of 15 parameters, including E_0, the photoelectron threshold energy. The refined parameters (excluding angular terms) are given in Tables 2 and 3 in bold type.

[1] XAFS refers collectively to EXAFS and XANES combined.

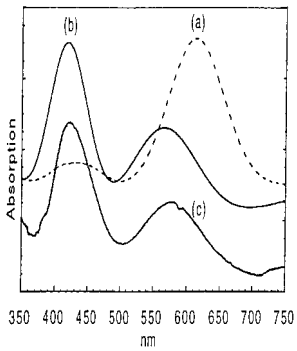

FIGURE 1: Optical absorption spectra of Met121Glu: (a) pH 4, (b) pH 8, and (c) the azide complex at pH 8.

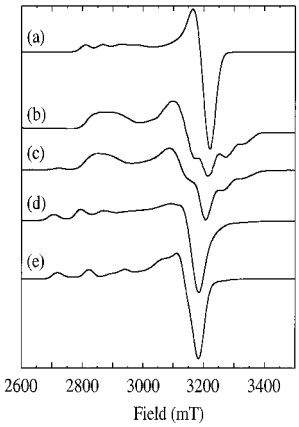

FIGURE 2: X-Band EPR spectra of frozen solutions of (a) Az_p at pH 8, (b) stellacyanin at pH 7, (c) the Met121Glu mutant at pH 4, (d) the Met121Glu mutant at pH 8, and (e) the Met121Glu mutant with azide at pH 8.

RESULTS

Optical Spectrum

Figure 1 shows the optical absorption spectrum of the Met121Glu mutant at two pH values (a and b) together with the optical spectrum for the azido derivative at pH 8 (c). The Met121Glu mutant exhibits an intense band at pH 4 at 614 nm ($\epsilon = 4500$ M^{-1} cm^{-1}; Karlsson et al., 1991) and a weaker band at 450 nm. These bands are similar in intensity and position to the optical spectrum of stellacyanin and to optical data for other methionine mutants of azurin which exhibit rhombic EPR spectra (Murphy et al., 1993). As the pH is increased, both optical bands shift toward shorter wavelengths. Thus, at pH 8, bands appear at 570 and 413 nm, the latter becoming the more intense of the two with an ϵ of 2500 M^{-1} cm^{-1}, signifying a major alteration in the S(Cys)σ > Cu($d_{x^2-y^2}$) overlap. Addition of azide results in only small changes in this spectrum.

EPR Spectroscopy

Figure 2 shows X-band EPR spectra at 77 K of the Met121Glu mutant at pH 4 and 8 together with native azurin at pH 8. Also shown is the EPR spectrum of the azide derivative of Met121Glu recorded at pH 8. Spectra were simulated for Met121Glu. The EPR spectrum of Az_p shows small changes with pH (Groeneveld et al., 1987) and is typical of that group of small blue copper proteins which possess an axial spectrum and a narrow hyperfine splitting in the $g_{||}$ region. In contrast, the spectrum for Met121Glu at pH 4 is rhombic, similar to that found for stellacyanin

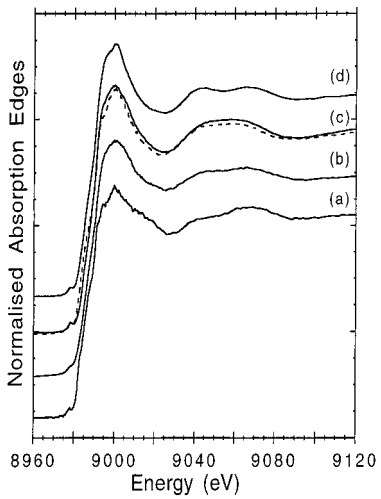

FIGURE 3: Normalized X-ray absorption near edge structure (XANES) for the Cu(II) site in (a) Az_p at pH 8, (b) stellacyanin at pH 7, (c) the Met121Glu mutant and the azide complex (dashed line) at pH 8, and (d) the Met121Glu mutant at pH 4.

(Malmstrom et al., 1970), which is also shown in Figure 2. The EPR parameters at pH 8 are similar to those reported for the type 2 Cu center of blue nitrite reductase from *Alcaligenes xylosoxidans*, which has an $A_{||}$ of 90 G and a $g_{||}$ of 2.35 (Howes et al., 1994). For the azide-bound derivative, there is a further increase in hyperfine splitting to 110 G and a reduction in the $g_{||}$ by 0.05, indicating a significant rearrangement of the Cu site from a typical type 1 Cu site.

EXAFS Data and Structural Interpretation

Figure 3 shows the normalized X-ray absorption edge data for the Cu(II) oxidation states of the Met121Glu mutant at pH 4 and 8. The latter is compared to the spectrum for the azido derivative (shown as a dashed line). Also shown for comparison are the absorption edges for the native protein at pH 8 and stellacyanin at pH 7. The edges show a number of relatively broad features, but differences between them may be discerned. The edges of Met121Glu and stellacyanin are more similar to each other than to that of Az_p. The XANES spectrum of the azido derivative is sufficiently different from that of oxidized Met121Glu at high pH to indicate that azide binding results in some rearrangement of the Cu site ligation and/or geometry.

The Cu K-edge EXAFS data for Cu(II) Met121Glu at pH 4 and 8 are shown in Figure 4 together with their respective Fourier transforms. The data clearly show that a major change in the copper environment occurs at high pH; the higher overall frequency of the EXAFS at pH 8 suggests a small increase in the inner shell radius, as indicated by the first peak in the Fourier transform. In the following sections, detailed analyses of the data are presented to quantify the changes involving the copper ligands and to determine which are responsible for the observed spectroscopic effects.

(A) Met121Glu at pH 4. The EXAFS and Fourier transforms of the Met121Glu spectrum compare very closely to those of the End-121, which also has a rhombic EPR spectrum [not shown here, see Murphy et al. (1993)]. Thus, the starting model was based upon the parameters obtained for the End-121 mutant (Murphy et al., 1993), which consisted of an inner shell of 2N(His) at 1.93 Å, 1S(Cys) at 2.15 Å, and 1O at 2.26 Å, which was tentatively assigned to a water molecule in the End-121 mutant. The outer shell

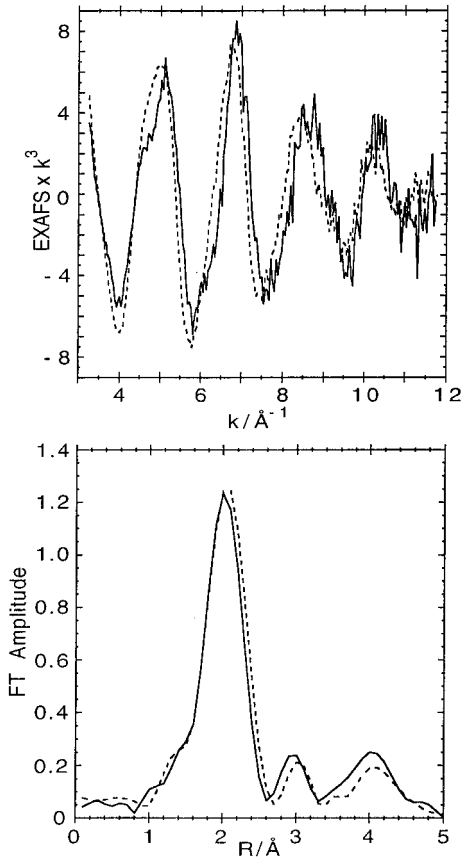

FIGURE 4: EXAFS and Fourier transforms of the Met121Glu mutant: pH 4 (solid line) and pH 8 data (dashed line) compared.

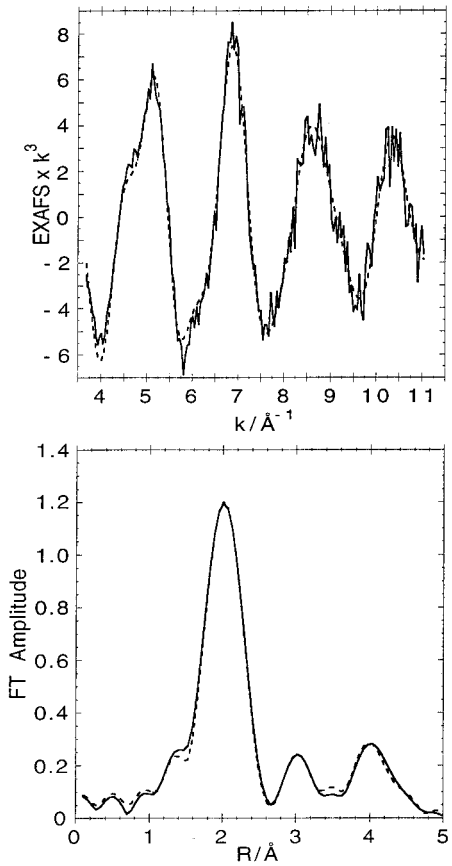

FIGURE 5: Simulation of EXAFS of the Met121Glu mutant at pH 4 (experiment is solid line; theory is dashed line).

Table 1: EPR Parameters[a] for Az_p (pH 5.2), Stellacyanin (pH 1−9), Met121Glu (pH 4 and 8), Met121Glu with Azide (pH 8), and the Type 2 Cu Site of *A. xylosoxidans* Nitrite Reductase (pH 7.4)

protein	pH	g_x	g_y	g_z	A_x	A_z
Az_p[b]	5.2	2.035	2.052	2.263	53	
St[c]	1−9	2.025	2.077	2.287	60	34
Met121Glu	4	2.03	2.085	2.30	65	25
Met121Glu	8	2.06	2.06	2.30	10	83
Met121Glu azide	8	2.06	2.06	2.25	10	110
*Ax*NiR[d]	7.4	2.038	2.038	2.355	−	90

[a] The hyperfine couplings are in gauss. [b] Groeneveld et al. (1987). [c] Malmström et al. (1970). [d] Howes et al. (1994).

Table 2: Parameters Used To Simulate the Cu(II) K-Edge EXAFS of Met121Glu at pH 4

shell	atoms	R (Å)	$2\sigma^2$ (Å^2)
1	2N(His)	**1.93**	**0.003**
2	2C(His)	2.86	**0.007**
3	2C(His)	3.01	0.007
4	2N(His)	4.03	**0.013**
5	2C(His)	4.12	0.013
6	1S(Cys)	**2.15**	**0.000**
7	1O	**2.86**	0.017
8	2C	**3.27**	**0.021**
	FI = 0.33, R = 19.6%, E_0 = **20.97** eV		

atoms consisted of the remaining histidine atoms, an oxygen at 2.86 Å, and 2C at 3.26 Å (Murphy et al., 1993). This model, when applied to the Met121Glu at pH 4 data, resulted in an FI of 0.46 and an *R* factor of 25.0%. An improvement to the fit was obtained by removing the oxygen shell at 2.26 Å (FI = 0.40, R = 22.0%). The inner shell copper coordination in this model consists of 2N(His) at 1.93 Å (α = 0.003 Å^2) and 1S(Cys) at 2.15 Å (α = 0.000 Å^2). The presence of the additional low-Z atoms, which refined to 1O at 2.86 Å (α = 0.017 Å^2) and 2C at 3.27 Å (α = 0.021 Å^2), reduced the final fit index to 0.33 and *R* factor to 19.6% (Figure 5, Table 2). During the course of this work, the crystal structure parameters for Met121Glu at low pH have become available and are given in Table 4 (Karlsson et al., 1996). The pH of the crystals used has been estimated to be approximately 4 from resonance Raman spectroscopy. A simulation of the EXAFS based upon these parameters [2N(His) at 2.01 Å, 1S(Cys) at 2.11 Å, and 1O at 2.21 Å] resulted in a very poor fit (FI = 1.59, R = 47.8%). Refinement resulted in the shortening of the Cu−N(His) and Cu−S(Cys) distances, refining to 1.93 Å (α = 0.003 Å^2) and 2.15 Å (α = 0.000 Å^2), respectively. These refined distances are the same as those obtained when the starting values were taken from the End-121 model, thus providing strong support for the correctness of these distances in solution. The oxygen refined to 2.29 Å but with a very high Debye−Waller term (α = 0.03 Å^2), suggesting that it was not essential to the fit. As in the simulation based on the End-121 model, the additional low-Z atoms refined to 1O at 2.86 Å (α = 0.017 Å^2) and 2C at 3.27 Å (α = 0.021 Å^2).

(B) Met121Glu at pH 8. Figure 4 shows a major change in the copper site structure as the pH is increased. The overall frequency of the EXAFS pattern has changed, indicating a significant difference in the copper site structure of the mutant with pH. Detailed analysis of the high-pH Met121Glu EXAFS data shows that a fourth low-Z atom is required in the inner coordination sphere in addition to the 2N(His) and 1S(Cys) atoms. This atom is assumed to be an oxygen from the glutamate ligand, and refinement shows it to be the closest ligand to the copper. In the final

Table 3: Parameters Used to Simulate the Cu(II) K-Edge EXAFS of (a) Met121Glu at pH 8 and (b) Met121Glu with Azide at pH 8[a]

	shell	atoms	R (Å)	$2\sigma^2$ (Å^2)
(a)	1	2N(His)	**2.00**	**0.005**
	2	2C(His)	2.93	**0.008**
	3	2C(His)	3.07	0.008
	4	2N(His)	4.10	**0.016**
	5	2C(His)	4.18	0.016
	6	1S(Cys)	**2.21**	**0.003**
	7	1O(Glu)	**1.90**	**0.003**
	8	1O(Glu)	2.86	**0.004**
	9	1C(Glu)	3.26	**0.008**
	10	1C(Glu)	3.78	**0.011**
		FI = 0.17, R = 15.1%, E_0 = **20.97** eV		
(b)	1	2N(His)	**1.99**	**0.005**
	2	2C(His)	2.91	**0.009**
	3	2C(His)	3.07	0.009
	4	2N(His)	4.08	**0.018**
	5	2C(His)	4.17	0.018
	6	1S(Cys)	**2.20**	**0.003**
	7	1N(azide)	**1.91**	**0.005**
	8	1N(azide)	2.79	**0.008**
	9	1N(azide)	3.81	**0.025**
		FI = 0.41, R = 20.1%, E_0 = **22.37** eV		

[a] Omitting the outer shell atoms of glutamate in part a gives an FI that is 59% worse; omitting the outer shell atoms of azide in part b gives an FI that is 13% worse.

simulation of the data, the glutamic acid ligand has been modeled as a single unit, consisting of the two oxygen atoms and two atoms of the C_α side chain. The remaining atoms of the glutamate side chain were found to be too distant from the copper atom to make any significant contribution to the EXAFS. The glutamate unit and the imidazole ring of the histidines were used in a constrained refinement. Initially, the histidine and glutamate were placed 1.95 Å from the copper with the S(Cys) at 2.15 Å. The best fit using these "average" Cu−N/O distances gave an FI of 0.31. Refinement led to a fit with the two histidines coordinated at 2.00 Å (α = 0.005 Å^2), the S(Cys) at 2.21 Å (α = 0.003 Å^2), and the O_ϵ(Glu) at 1.90 Å (α = 0.003 Å^2). The simulation gave an FI of 0.17 and an R of 15.1% (Figure 6). Thus, a considereble improvement in FI is seen for the glutamate coordinated at a shorter distance than histidine. The fit parameters are given in Table 3a.

(C) Azide Complex at pH 8. A simulation of the high-pH azide-bound derivative of Met121Glu is shown in Figure 7. The EPR data (figure 2) show a major change upon addition of azide, suggesting that azide strongly perturbs the Cu site. Four ligands provided by the two histidines, the cysteine, and a low-Z ligand were required to fit the spectrum. In the simulation shown, the fourth ligand was provided by an azide coordinated at 1.91 Å (α = 0.005 Å^2). This replaces the glutamate ligand which was present in the native high-pH simulation (B above). The azide molecule was included as a fixed scattering unit so that its position could be determined by a constrained multiple-scattering calculation. In the final simulation, the azide group is coordinated at an angle of 128°, which is normal for terminal azide binding to copper (Blackburn et al., 1987, and references therein). The fit parameters gave an FI of 0.41 and an R of 20.1% and are given in Table 3b. Attempts to fit a Cu−O(Glu) did not provide a convincing minimum. Two possible minima were found with Cu−O(Glu) distances of 2.4 and 3.25 Å. In each case, the fit index was larger than in the absence of this ligand. It is probable that the Glu side chain is no longer coordinated directly to Cu when azide is bound and its contribution to the EXAFS is too weak to be seen.

DISCUSSION

A summary of the main EXAFS fit parameters for Cu(II) Met121Glu are shown in Table 4 together with the corresponding information for Az_p (Murphy et al., 1993) and crystallographic data for Met121Glu at 2.3 Å resolution (Karlsson et al., 1996). High-resolution crystallographic data for Az_p (pH 9.0) at 1.93 Å (Nar et al., 1991), azurin II from *A. xylosoxidans* (AzII) at 1.90 Å (Dodd et al., 1995), and *Populus nigra* plastocyanin at 1.33 Å (Guss et al., 1992) are included in the table for comparison. The crystallographic parameters of the plastocyanin are included as this perhaps provides the most accurate metrical information around the Cu site among the crystallographically characterized blue Cu proteins [see Guss et al. (1992) for a more full discussion].

The discrepancy between the actual values for the different Cu−ligand distances for azurin from the two techniques has already been discussed earlier (Murphy et al., 1993; Dodd et al., 1995). In particular, the Cu−His and Cu−Cys distances in the crystallographic structure of Az_p (Nar et al., 1991) are systematically longer than the EXAFS-derived values. The Cu−Cys distance in the crystal structure of Az_p (Nar et al., 1991) is significantly longer than that in the crystal structures of AzII (Dodd et al., 1995) and azurin from *Alaligenes denitrificans* AzAD (Baker, 1988), the only two other azurins for whom crystallographic structures have been refined to high resolution. The Cu−Cys distance in 1.33 Å Pc (Guss et al., 1992) structure is similar to that in AzII and AzAD, thus making the Az_p distance exceptional. The Cu−S(Cys) for Az_p (Nar et al., 1991) is also longer than the EXAFS value of Az_p in solution (Murphy et al., 1990). We also note that the average Cu−His distances are longer in the case of AzAD (0.11 Å), Az_p (0.15 Å), and AzII (0.10 Å) compared to the EXAFS value for Az_p. The 1.33 Å refined structure of plastocyanin (Guss et al., 1992) shows an excellent agreement has been found with the metrical information obtained from EXAFS data of solution (Murphy et al., 1991) and single-crystal (Scott et al., 1982) plastocyanin. We note that EXAFS data for the Cu−His and Cu−Cys distances are expected to be accurate to within ±0.03 Å. The differences discussed above are similar to what would be expected for one electron oxidation/reduction step. For example, in rubredoxin, one electron reduction causes a lengthening of the Fe−S bonds by ∼0.06 Å (Teo & Shulman, 1982), and in plastocyanin, a similar lengthening has been observed in Cu−His and Cu−Cys bonds (Murphy et al., 1991). Thus, it is important to establish the accuracy of this metrical information from chemical and functional points of view.

The difficulties in assessing the true errors for the metal−ligand distances in a crystallographic study of a metalloprotein have already been discussed in some detail (Guss et al., 1992; Dodd et al., 1995). The classical Luzatti (1952) plot provides a conservative estimate for an overall accuracy of a structure at a given resolution. For azurins, comparison of coordinates for independent molecules in the asymmetric unit of a crystal has been made in order to assess the errors in the metal−ligand distances (Baker, 1988; Nar et al., 1991).

Table 4: Cu(II) Coordination in Azurin from *Pseudomonas aeruginosa* and *A. xylosoxidans*, Glu-121 Mutant, and *Populus nigra* Plastocyanin[a]

	crystallographic[b]				XAFS[c]			
					Az_p	Glu-121		
	Az_p pH 9 1.93 Å[f]	AzII pH 6 1.90 Å[f]	Pc[d] pH 6 1.33 Å (1.6 Å)[f]	Glu-121 pH 4 2.3 Å[f]	pH 8	pH 4	pH 8	azide
Cu−S (Cys)	2.25	2.12	2.07 (2.13)	2.11	2.12 (0.000)	2.15 (0.000)	2.21 (0.003)	2.20 (0.003)
Cu−N (His)	2.03 2.11	2.02 2.02	1.91 (2.04) 2.06 (2.10)	2.01 2.01	1.93 1.93 (0.005)	1.93 1.93 (0.003)	2.00 2.00 (0.005)	1.99 1.99 (0.005)
Cu−O[e]	2.97	2.75	−	3.42	2.79 (0.014)	2.86 (0.017)	2.86 (0.004)	2.79 (0.008)
Cu−S (Met)	3.15	3.26	2.82 (2.90)	−	3.04	−	−	−
Cu−O (Glu)	−	−	−	2.21	−	−	1.90 (0.003)	−
Cu−N (azide)	−	−	−	−	−	−	−	1.91 (0.005)

[a] Distances and are in Å; numbers in parentheses are Debye−Waller terms ($2\sigma^2$) in Å^2. [b] Az_p data from Nar et al. (1991), Glu-121 data from Karlsson et al. (1996); and data for azurin II from *A. xylosoxidans* NiR from Dodd et al. (1995). [c] Data for Az_p from Murphy et al. (1993). [d] Data for oxidized platocyanin from *P. nigra* from Guss et al. (1993); the Cu−ligand bond lengths are given for the refined structure at 1.33 Å with the same parameters refined at 1.66 Å resolution in brackets. [e] Oxygen from glycine for Az_p and AzII, oxygen from glutamate for Glu-121 at pH 8.0, and nitrogen from azide in the Glu-121 azide complex (see text for details). [f] Crystal structure resolution.

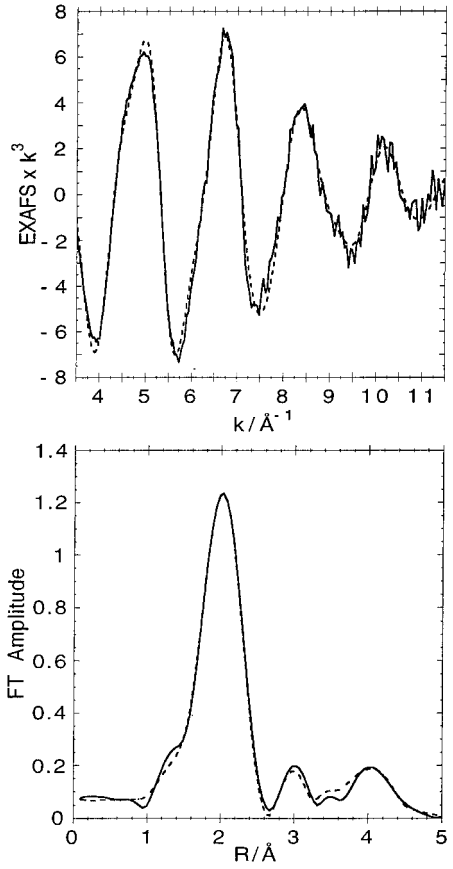

FIGURE 6: Simulation of EXAFS of the Met121Glu mutant at pH 8 (experiment is solid line; theory is dashed line).

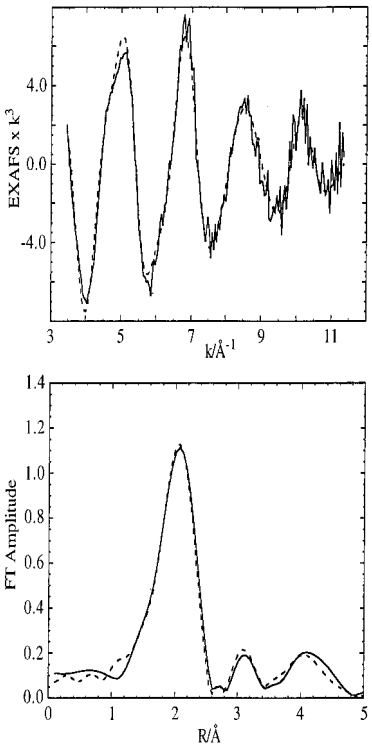

FIGURE 7: Simulation of EXAFS of the Met121Glu mutant with azide at pH 8 (experiment is solid line; theory is dashed line).

However, as noted by Guss et al. (1992), this approach can only provide the self-consistency of the structure but cannot be used for estimating errors of metal−ligand distances as a variety of systematic errors could effect each of the molecules in the crystal. Guss et al. (1992) have undertaken a comprehensive study on the refinement of plastocyanin at 1.33 Å resolution with the aim of assessing errors in metal−ligand distances in such structure determinations. They observed that in their 1.33 Å refinement all four Cu−ligand distances were systematically shorter than in the 1.6 Å refined stucture and were in good agreement with EXAFS results (Scott et al., 1982; Murphy et al., 1991). The exact reasons for this shortening are not fully understood as several factors affected the metal−ligand distances in the two refinements [Guss et al., 1992; also see Fields et al. (1994)]. However, Guss et al. have provided some guidance for uncertainties in such determinations and have estimated uncertainties in metal−ligand distances of ±0.04 and ±0.07 Å for well-refined structures of a small ∼10 kDa protein at 1.3 and 1.8 Å resolution, respectively.

The pK_a value of the pH dependence observed in optical and EPR spectra of Met121Glu is very close to 5 (Karlsson et al., 1996). The pH values at which the EXAFS measurements were made ensured that essentially only a single species of copper binding site was present in each case. The EXAFS-derived parameters for the Cu(II) site of high-pH

Met121Glu are consistent with the optical and EPR data, which show a change from normal type 1 copper coordination at low pH to a new form of copper-bound protein at high pH. The distance of the histidine ligands (2.00 Å) is 0.07−0.11 Å longer than that in the low-pH data as well as those in the EXAFS of Az_p, Asp-121, End-121, and other type 1 copper proteins, such as stellacyanin [Table 4; see also Murphy et al. (1993), Strange et al. (1995a), and Lommen et al. (1991)]. Instead, the Cu−N(His) distance found for high-pH Met121Glu is similar to some of the "nonblue" catalytic copper sites in proteins which possess four strong bonds [e.g. Blackburn et al. (1987, 1992), Knowles et al. (1989), and Scott et al. (1988)] and in Cu(II)−imidazole model compounds [e.g. Strange et al. (1987) and Orpen et al. (1989)]. There is also a lengthening of the Cu(II)−S(Cys) bond of about 0.06 Å in going from pH 4 to 8, consistent with the increase in copper coordination. The increased distance of the S(Cys) will reduce the overlap with the Cu and hence the decreased intensity of the 600 nm band. Furthermore, a strong linkage of Cu−O_ϵ1, accompanied by an increased histidine distance of 2.00 Å, suggests a movement of the metal ion from the trigonal plane toward the oxygen, leading to a significant rearrangement of the site geometry, consistent with the much increased hyperfine coupling in the EPR spectrum. The similarity of the EPR parameters at pH 8 to those of the catalytic Cu center of the blue NiRs from *A. xylosoxidans* (Howes et al., 1994), *Pseudomonas aureofaciens* (Zumft et al., 1987), and *Hyphomicrobium* (Suzuki et al., 1993) may suggest a correspondence in Cu site symmetry. There is no crystal structure for any of the blue NiRs, but the crystal structures of the green NiRs from *Alcaligenes faecalis* (Kukimota et al., 1994) and *A. cycloclastes* (Godden et al., 1991) show that the type 2 Cu site in both cases possesses an unusual nearly tetrahedral symmetry. However, the EPR spectra for these green NiRs show much larger values of $A_{||}$ for the type 2 Cu site: 151 G (Kukimota et al., 1994) and 165 G (Iwasaki et al., 1975), respectively.

Molecular modeling, assuming a rigid copper site, suggests that straightforward substitution of a glutamate residue for methionine-121 would place the O_ϵ1 atom about 2.4 Å from the copper (Karlsson et al., 1991). The crystal structure suggets that the copper atom moves 0.2 Å in the direction of the glutamate residue, and this movement reduces the Cu−Glu(O_ϵ1) distance to 2.2 Å. The EXAFS data suggest that an even larger movement of the copper toward the glutamate, at least 0.5 Å, must be allowed, that the glutamate side chain moves toward the copper, or that a combination of these two movements takes place, which allow the O_ϵ1 of Met121Glu at pH 8 to coordinate to Cu at 1.90 Å.

The O_ϵ1 contribution is absent from the EXAFS of the Met121Glu mutant at pH 4 (Table 4), suggesting that it is disordered and/or at a distance significantly longer than 2.3 Å with a consequence that its contribution to the EXAFS is too weak to be seen clearly. This is at variance with the crystal structure and may be due to a difference in pH in the crystal, even though resonance Raman spectroscopy indicates a pH of 4, or it may be a genuine difference between the crystal and solution. Thus, in solution at pH 4, two histidines and the cysteine alone form the primary ligands to the copper, with Cu−ligand distances similar to those determined from EXAFS data of other type 1 Cu centers. There is a longer oxygen shell at 2.86 Å. This shell could be assigned to the O_ϵ2 of the glutamic acid residue or possibly to Gly-45. A similar oxygen shell was observed in the Az_p, Asp-121 (pH 8), and End-121 and assigned to the Gly-45 ligand, in line with crystallographic data for the native protein (Murphy et al., 1993). We note that, in the crystallographic structure of this mutant, the distance to the carbonyl oxygen of Gly-45 is 3.4 Å (Karlsson et al., 1996).

The extent of the protonation of the glutamate side chain is important. At low pH, the glutamate will be protonated and evidently would form only a weak interaction, although strong enough to markedly change the optical absorbance spectrum and the EPR properties from an axial spectrum in the wild type to a rhombic spectrum in the mutant. At high pH (pH 8), the glutamate residue is deprotonated and charge may be donated to the copper atom. This would increase the strength of the Cu(II)−Glu(O_ϵ1) interaction and bring about movement of the copper atom toward the glutamate side chain, leading to a strong bond between them (see above). The pH-dependent spectroscopic changes observed for Met121Glu, thus, result from the reversible binding of the glutamate residue and the concomitant rearrangement of the other copper ligands. The movement of the copper atom toward the glutamate residue will also contribute to closer interaction.

At pH 8, the Met121Glu protein is different than native type 1 copper protein on the basis of the EXAFS analysis, in having a copper site with four strong ligands. Also, the EPR shows a hyperfine coupling similar to that of the catalytic "type 2" Cu site in the blue NiRs. It is thus likely that the site symmetries of the two are very similar in nature. However, the Met121Glu mutant at this pH may still be regarded as having a type 1 copper site since it maintains the minimum requirement of possessing a short Cu−S(Cys) bond and strong charge transfer bands in the visible region of the absorbance spectrum. But we note that the Cu−S(Cys) bond is significantly longer ($\geq$0.06 Å) compared to that of pH 4.0 and native Az_p, Pc, or other type 1 proteins which have been characterized by the EXAFS. Similar ligation is also maintained in the azide-bound form of Met121Glu when the hyperfine coupling increases still further to 110 G. For this complex, the space occupied by the glutamate ligand is presumably taken up instead by the azide anion. The EXAFS parameters (Table 3) indicate that the Cu−ligand distances are not altered significantly when azide is bound. However, the XANES data (Figure 3) do suggest a change in the Cu site geometry, and this observation is supported by the increase in the $A_{||}/g_{||}$ ratio for the azido derivative, consistent with a less distorted tetragonal symmetry at the Cu site compared to that for unligated high-pH Met121Glu.

It is obvious from this and other studies that the original classification of copper proteins based upon the optical and EPR properties is too simple and a re-examination is needed for a more sophisticated classification which not only takes account of the spectroscopic properties but also takes account of the detailed structure of the copper site, including bond distances, geometry, and the type of ligands.

REFERENCES

Adman, E. T. (1985) *Top. Mol. Struct. Biol*., 1−42.
Adman, E. T., & Jensen, L. H. (1981) *Isr. J. Chem. 21*, 8−12.
Baker, E. N. (1988) *J. Mol. Biol. 203*, 1071−1075.

Bergman, C., Gandvik, E.-K., Nyman, P. O., & Strid, L. (1977) *Biochem. Biophys. Res. Commun. 77*, 1052−1059.
Binsted, N., Cook, S. L., Evans, J., Greaves, G. N., & Price, R. J. (1987) *J. Am. Chem. Soc. 109*, 3669−3676.
Binsted, N., Gurman, S. J., Campbell, J. W., & Stephenson, P. (1991) *SERC Daresbury Laboratory Program EXCURVE*, Daresbury Laboratory, Warrington, U.K.
Binsted, N., Strange, R. W., & Hasnain, S. S. (1992) *Biochemistry 31*, 12117−12125.
Blackburn, N. J., Strange, R. W., McFadden, L. M., & Hasnain, S. S. (1987) *J. Am. Chem. Soc. 109*, 7162−7170.
Blackburn, N. J., Strange, R. W., Farooq, A., Haka, M. S., & Karlin, K. D. (1988) *J. Am. Chem. Soc. 110*, 4263−4272.
Blackburn, N. J., Strange, R. W., Carr, R. T., & Benkovic, S. J. (1992) *Biochemistry 31*, 5298−5303.
Canters, G. W. (1987) *Rec. Trav. Chim. Pays-Bas 106*, 6−7.
Dodd, F. E., Hasnain, S. S., Abraham, Z. H. L., Eady, R. R., & Smith, B. E. (1995) *Acta Crystallogr. D 51*, 1052−1064.
Fields, B. A., Guss, J. M., & Freeman, H. C. (1991) *J. Mol. Biol. 222*, 1053−1065.
Fields, B. A., Bartsch, H. H., Bartunik, H. D., Cordes, F., Guss, J. M., & Freeman, H. C. (1994) *Acta Crystallogr. D 50*, 709−730.
Godden, J. W., Turley, S., Teller, D. C., Adman, E. T., Liu, M. Y., Payne, W. J., & LeGall, J. (1991) *Science 253*, 438−442.
Gray, H. B., & Malmström, B. G. (1983) *Comments Inorg. Chem. 2*, 203−209.
Groeneveld, C. M., Aasa, R., Reinhammar, B., & Canters, G. W. (1987) *J. Inorg. Biochem. 31*, 143−154.
Grössman, J. G., Ingledew, W. J., Harvey, I., Strange, R. W., & Hasnain, S. S. (1995) *Biochemistry 34*, 8406−8414.
Gurman, S. J., Binsted, N., & Ross, I. (1984) *J. Phys. C: Solid State Phys. 17*, 143−151.
Gurman, S. J., Binsted, N., & Ross, I. (1986) *J. Phys. C: Solid State Phys. 19*, 1845−1861.
Guss, J. M., & Freeman, H. C. (1983) *J. Mol. Biol. 169*, 521−563.
Guss, J. M., Harrowell, P. R., Murata, M., Norris, V. A., & Freeman, H. C. (1986) *J. Mol. Biol. 192*, 361−387.
Guss, J. M., Merritt, E. A., Phizackerley, R. P., Hedman, B., Murata, M., Hodgson, K. O., & Freeman, H. C. (1988) *Science 241*, 806−811.
Guss, J. M., Bartunik, H. D., & Freeman, H. C. (1992) *Acta Crystallogr. B 48*, 790−811.
Hasnain, S. S. (1988) *Top. Curr. Chem. 147*, 73.
Howes, B. D., Abraham, Z. H. L., Lowe, D. J., Brüser, T., Eady, R. R., & Smith, B. E. (1994) *Biochemistry 33*, 3171−3177.
Iwasaki, H., Noji, S., & Shidara, S. (1975) *J. Biochem. 78*, 355−361.
Karlsson, B. G., Pascher, T., Nordling, M., Arvidsson, R. H. A., & Lundberg, L. G. (1989a) *FEBS Lett. 246* (1, 2), 211−217.
Karlsson, B. G., Aasa, R., Malmström, B. G., & Lundberg, L. G. (1989b) *FEBS Lett. 253* (1, 2), 99−102.
Karlsson, B. G., Nordling, M., Pascher, T., Tsai, L.-C., Sjölin, L., & Lundberg, L. G. (1991) *Protein Eng. 4* (3), 343−349.
Karlsson, B. G., Tsai, L.-C., Nar, H., Sanders-Loehr, J., Bonander, N., Langer, V., & Sjolin, L. (1996) *Biochemistry* (submitted for publication).
Knowles, P. F., Strange, R. W., Blackburn, N. J., & Hasnain, S. S. (1989) *J. Am. Chem. Soc. 111*, 102−107.
Kukimota, M., Nishiyama, M., Murphy, M. E. P., Turley, S., Adman, E. T., Horinouchi, S., & Beppu, T. (1994) *Biochemistry 33*, 5246−5252.
Lommen, A., Pandya, K. I., Koningsberger, D. C., & Canters, G. W. (1991) *Biochim. Biophys. Acta 1076*, 439−447.
Luzatti, V. (1952) *Acta Crystallogr. 5*, 802−810.
Malkin, R., & Malmström, B. G. (1970) *Adv. Enzymol. 33*, 177−244.
Malmström, B. G., Reinhammar, B., & Vänngård, T. (1970) *Biochim. Biophys. Acta 205*, 48−57.
Morrell, C., Baines, J. T. M., Campbell, J. W., Diakun, G. P., Dobson, B. R., Greaves, G. N., & Hasnain, S. S. (1989) EXAFS Users' Manual, Daresbury Laboratory, Warrington, U.K.
Murphy, L. M., Hasnain, S. S., Strange, R. W., Harvey, I., & Ingledew, W. J. (1991) in *X-Ray Absorption Fine Structure* (Hasnain, S. S., Ed.) pp 152−155, Ellis-Horwood, Chichester, U.K.
Murphy, L. M., Strange, R. W., Karlsson, G., Lundberg, L., Pascher, T., Reinhammar, B., & Hasnain, S. S. (1993) *Biochemistry 32*, 1965−1975.
Nar, H., Messerschmidt, A., Huber, R., van de Kamp, M., & Canters, G. W. (1991) *J. Mol. Biol. 221*, 765−772.
Norris, G. E., Anderson, B. F., & Baker, E. N. (1986) *J. Am. Chem. Soc. 108*, 2784−2785.
Orpen, A. G., Brammer, L., Allen, F. H., Kennard, O., Watson, D. G., & Taylor, R. (1989) *J. Chem. Soc., Dalton Trans. Suppl.*, S1−S83.
Scott, R. A., Hahn, J. E., Doniach, S., Freeman, H. C., & Hodson, K. O. (1982) *J. Am. Chem. Soc. 104*, 5364−5369.
Scott, R. A., Sullivan, R. J., De Wolfe, W. E., Dolle, R. E., & Kruse, L. I. (1988) *Biochemistry 27*, 5411−5417.
Strange, R. W., Blackburn, N. J., Knowles, P. F., & Hasnain, S. S. (1987) *J. Am. Chem. Soc. 109*, 7157−7162.
Strange, R. W., Reinhammar, B., Murphy, L. M., & Hasnain, S. S. (1995a) *Biochemistry 34*, 220−231.
Strange, R. W., Dodd, F. E., Abraham, Z. H. L., Grössmann, J. G., Brüser, T., Eady, R. R., Smith, B. E., & Hasnain, S. S. (1995b) *Nat. Struct. Biol. 2* (4), 287−292.
Suzuki, S., Kohzuma, T., Shidara, S., Okhki, K., & Aida, T. (1993) *Inorg. Chim. Acta 208*, 107−109.
Teo, B. K., & Shulman, R. G. (1982) in *Iron-sulfur proteins* (Spiro, T. G., Ed.) Chapter 9, John Wiley.
Thomann, H., Bernardo, M., Baldwin, M. J., Lowery, M. D., & Solomon, E. I. (1991) *J. Am. Chem. Soc. 113*, 5911.
van de Kamp, M., Hali, F. C., Rosato, N., Finazzi Agro, A., & Canters, G. W. (1990) *Biochim. Biophys. Acta 1019*, 283−292.
Zumft, W. G., Gotzmann, D. J., & Kroneck, P. M. H. (1987) *Eur. J. Biochem. 168*, 301−307.

BI961682Z